Simple Mixing Criteria for the Growth of Negatively Buoyant Phytoplankton
Author(s): Katherine R. O'Brien, Gregory N. Ivey, David P. Hamilton, Anya M. Waite and Petra M. Visser
Source: *Limnology and Oceanography,* Vol. 48, No. 3 (May, 2003), pp. 1326-1337
Published by:
Stable URL: http://www.jstor.org/stable/3096659
Accessed: 22-12-2015 23:49 UTC

http://www.jstor.org

Simple mixing criteria for the growth of negatively buoyant phytoplankton

Katherine R. O'Brien,[1] Gregory N. Ivey, David P. Hamilton,[2] and Anya M. Waite
Centre for Water Research, University of Western Australia, Crawley, Western Australia, 6009, Australia

Petra M. Visser
Aquatic Microbiology, Institute for Biodiversity and Ecosystem Dynamics, University of Amsterdam,
Nieuwe Achtergracht 127, 1018 WS Amsterdam, The Netherlands

Abstract

Phytoplankton population dynamics are controlled by the relative rather than absolute timescales of mixing, growth, and loss processes such as sedimentation, grazing, and so on. Here, the vertical distribution and biomass of phytoplankton populations are quantified by two timescale ratios: the Peclet number Pe—the ratio of mixing and sedimentation timescales—and the growth number G—the ratio of sedimentation and net growth timescales. Three mixing regimes are defined for phytoplankton and other particles. For Pe $\geq$ 100, the population is translated linearly down the water column over time and will leave the surface mixing layer completely after sedimentation time τ_s. For 0.1 < Pe < 100, the population distribution depends on the relative magnitude of Pe and G. Finally, for Pe $\leq$ 0.1, the population will be vertically uniform, and biomass changes exponentially over time with characteristic timescale $\tau_c = \tau_s/(G - 1)$. This analysis is valid for negatively buoyant phytoplankton, except when mixing time is much longer than growth time and Pe $\leq$ 0.1, which can occur for very slow sinking species. These regimes can be used for assessing the effect of changes in the mixing, growth, or sedimentation conditions on population dynamics. Published data from a lake and diurnally stratified river weir pool are used here to verify a minimum thermocline depth hypothesis proposed by others. Mixing and growth regimes are used to calculate minimum mixing depth h_{min} and to determine phytoplankton sinking rates from published sediment trap data.

The interaction between turbulent mixing and sedimentation determines the vertical distribution of negatively buoyant phytoplankton populations (Humphries and Lyne 1988; Ruiz et al. 1996; Reynolds 1998), which in turn affects resource availability and hence phytoplankton growth (Sverdrup 1953; Reynolds 1984; Walsby 1997; Huisman et al. 2002a). A population will not grow over time unless gross production exceeds all losses, including sedimentation, which is the focus of this paper. Hence, a population of negatively buoyant phytoplankton will not grow unless the growth number, G, given by the ratio of the sedimentation timescale to the net growth timescale, exceeds unity (Condie and Bormans 1997). If mixing is "too shallow," the population is limited by sedimentation losses (Visser et al. 1996b; Condie and Bormans 1997; Huisman and Sommeijer 2002b), and if mixing is "too deep," the population is limited by respiration and other losses (Sverdrup 1953; Smetacek and Passow 1990; Huisman et al. 2002a).

The one-dimensional form of the reaction-advection-diffusion equation quantifies the effect of sedimentation losses, phytoplankton growth, and turbulent mixing on the concentration and vertical distribution of phytoplankton (e.g., Okubo 1980). The equation can be solved numerically (e.g., Koseff et al. 1993; Bormans and Condie 1998; Lucas et al. 1998; Huisman and Sommeijer 2002b). Although full analytical solutions exist, they are complex and restricted to certain boundary conditions (Ruiz 1996; Ebert et al. 2001). However, the reaction-advection-diffusion equation converges to simple analytical solutions at very large or very small values of the Peclet number, Pe, which is the ratio of mixing time to sedimentation time (e.g., Smith 1982; Martin and Nokes 1988; Ruiz 1996; Condie and Bormans 1997). The Peclet number, Pe, and growth number, G, have been used in many forms to qualitatively describe phytoplankton dynamics and to explore different mixing, growth, sedimentation, and grazing scenarios (e.g., Spigel and Imberger 1987; Humphries and Lyne 1988; Ruiz et al. 1996; Condie and Bormans 1997; MacIntyre 1998). Here, Pe defines mixing regimes, which identify when simple analytical approximations can be used in place of the full reaction-advection-diffusion equation, without compromising the accuracy of predictions of phytoplankton biomass and vertical distribution. Growth regimes are defined in terms of both Pe and G.

Growth regimes have previously been determined from the reaction-advection-diffusion equation for sinking rate and growth parameters of a given species (Huisman et al. 1999, 2002a; Huisman and Sommeijer 2002b). This paper illustrates the merits and limitations of using dimensionless parameters and shows how they relate to the dimensional growth regimes of Huisman and Sommeijer (2002b).

Sedimentation of phytoplankton from the pelagic represents a significant export of carbon to the benthos (e.g., Hill 1992; Waite et al. 1992). Both sedimentation fluxes and phy-

Table 1. Summary of variables used in this text.

Variable	Description	Units
C	Concentration of phytoplankton	mg m^{-3}
C_0	Initial depth-integrated concentration	mg m^{-2}
$C_z(t)$	Depth-integrated concentration $= \int_0^h C(z, t) \, dz$	mg m^{-2}
G	Growth number, $\tau_s/\tau_g = \bar{\mu}_{net}h/w_s$	
h	Surface mixing layer depth	m
h_m	Maximum daily mixing depth	m
h_{min}	Minimum critical mixing depth	m
I	Irradiance (photosynthetically active radiation)	$\mu\varepsilon$ m^{-2} s^{-1}
I_0	Incident irradiance	$\mu\varepsilon$ m^{-2} s^{-1}
I_k	Half-saturation irradiance	$\mu\varepsilon$ m^{-2} s^{-1}
K_z	Vertical eddy viscosity	m^2 s^{-1}
K_{zp}	Vertical eddy diffusivity for particles	m^2 s^{-1}
ℓ	Characteristic turbulent length scale	m
NS	Net sedimentation	mg m^{-2}
Pe	Peclet number, $\tau_{mix}/\tau_s = w_sh/K_z$	
Pe$_p$	Particle Peclet number, $\tau_{mix}/\tau_s = w_sh/K_{zp}$	
RNS	Net relative sedimentation, NS/C_z	
SR	Sedimentation rate	mg m^{-2} s^{-1}
t	Time	s
w_{rms}	Root mean square (rms) of vertical turbulent velocity	m s^{-1}
w_s	Phytoplankton sinking rate	m s^{-1} or m d^{-1}
z	Depth, defined positive down	m
z_{eu}	Euphotic zone depth	m
z_s	Sediment trap deployment depth	m
z_{Tmin}	Minimum thermocline depth for positive growth	m
β	Constant used to determine Pe$_p$	
$\bar{\mu}_{net}$	Net depth-averaged daily growth rate	s^{-1} or d^{-1}
τ_c	Characteristic time for biomass growth or decay	s or d
τ_g	Growth time $= 1/\bar{\mu}_{net}$	s or d
τ_{mix}	Mixing time $= h^2/K_z$	s or d
τ_s	Sedimentation time $= h/w_s$	s or d
ζ	Variable transformation used to solve Eq. 2, $\zeta = z + w_st$	m

toplankton sinking rates can be estimated from sediment traps (e.g., Riebesell 1989; Visser et al. 1996b). If Pe $\ll$ 1 and $G \ll 1$, sinking rate can be calculated from sedimentation using simple expressions (e.g., Riebesell 1989; Ruiz 1996). Simple models also exist for systems where Pe $\ll$ 1 and $G \sim 1$ (Visser et al. 1996b) and where Pe is variable and $G \ll 1$ (Ruiz et al. 1996). A general framework is developed here for simple models of sedimentation as a function of sinking rate w_s for different mixing regimes, defined in terms of Pe, and for different values of G. Simple analytical models demonstrate the effect of mixing regime on sediment trap results, using published data from Lake Nieuwe Meer and mesocosm experiments with *Scenedesmus*.

The criteria for minimum mixing for growth of negatively buoyant phytoplankton in a surface mixing layer introduced by Huisman and Sommeijer (2002b) are redefined in terms of Pe, rather than turbulent eddy diffusivity K_z, and are tested using published data for negatively buoyant phytoplankton in two freshwater systems. The minimum mixing depth, h_{min}, is modeled for *Scenesdesmus* sp. in Lake Nieuwe Meer, The Netherlands, where mixing depth varied over timescales longer than 1 d (Visser et al. 1996a,b), and for the freshwater diatom *Aulacoseira granulata* in a diurnally stratified pool on the Murrumbidgee River, Australia (Webster et al. 1996; Bormans and Condie 1998; Sherman et al. 1998). Predic-

tions of h_{min} are compared with field data for biomass and surface mixing layer depth.

Modeling vertical distribution of phytoplankton

The mixing time $\tau_m = h^2/K_z$ (*see Table 1* for a summary of the variables used in the text) is the time for a tracer to become mixed through a surface mixing layer (SML) of depth h and vertical eddy diffusivity K_z (Tennekes and Lumley 1994). For phytoplankton sinking at rate w_s, the corresponding sedimentation time τ_s is simply h/w_s. The Peclet number Pe is defined by the ratio of mixing time to sedimentation time (Eq. 1).

$$\text{Pe} = \frac{\tau_m}{\tau_s} = \frac{w_sh}{K_z} \tag{1}$$

In a SML where the characteristic length scale ℓ of the turbulence scales according to depth h, and where w_{rms} is the root mean square (rms) of the vertical turbulent velocity fluctuations, the vertical eddy diffusivity can be parameterized as $K_z \sim w_{rms}\ell \sim w_{rms}h$ (Tennekes and Lumley 1994). The Peclet number is then equivalent to the ratio of the two velocity scales (Pe $= w_s/w_{rms}$). This velocity ratio is used by many authors as a surrogate for the Peclet number (e.g.,

Humphries and Lyne 1988; Martin and Nokes 1988; Webster and Hutchinson 1994).

For phytoplankton in a water column of zero mean flow, where the population can be represented by a horizontal average, the time-varying vertical concentration $C(z, t)$ at depth z and time t can be defined by the reaction-advection-diffusion equation

$$\frac{\partial C(z, t)}{\partial t} + w_s \frac{\partial C(z, t)}{\partial z}$$

$$= \mu_{net}(z, t)C(z, t) + \frac{\partial}{\partial z}\left[K_{zp}(z, t)\frac{\partial C(z, t)}{\partial z}\right] \quad (2)$$

where K_{zp} is the vertical eddy diffusivity of the phytoplankton, and μ_{net} is the net growth rate, including all loss processes except sedimentation (cf. Reynolds 1984; Visser et al. 1996b; Condie and Bormans 1997). Assuming no resuspension of phytoplankton leaving the base of the surface mixing layer, this problem can be described with a closed top boundary and an open bottom boundary condition (e.g., Koseff et al. 1993).

$$w_s C(z, t) - K_{zp}(z, t)\frac{\partial C(z, t)}{\partial z} = 0 \quad \text{for } z = 0$$

$$\frac{\partial C(z, t)}{\partial t} + w_s \frac{\partial C(z, t)}{\partial z} = \mu_{net}C(z, t) \quad \text{for } z = h \quad (3)$$

For Pe $\ll$ 1, phytoplankton will be uniformly distributed in the vertical (Martin and Nokes 1988), and $\mu_{net}(z, t)$ can be replaced by the net depth-averaged daily growth rate, $\bar{\mu}_{net}$, with a corresponding timescale $\tau_g = \bar{\mu}_{net}^{-1}$. This is a valid assumption unless $\tau_g/\tau_{mix} \ll 1$, which can lead to variations in the vertical profile. By introducing nondimensional parameters and neglecting terms with the coefficient Pe, Eqs. 2 and 3 reduce to (e.g., Condie and Bormans 1997)

$$\frac{dC(t)}{dt} = \left(\bar{\mu}_{net} - \frac{w_s}{h}\right)C(t) \quad (4)$$

Equation 4 can be solved and integrated over depth to yield the exponential model

$$C_z(t) = C_0 e^{[\bar{\mu}_{net} - (w_s/h)]t} \quad (5)$$

where $C_0 = C_z(0)$ is the initial value of the depth-integrated concentration C_z.

If Pe $\gg$ 1, this implies that the advection term in Eq. 2 is large compared to the mixing term. In this case, application of the boundary conditions (Eq. 3) leads to derivation of the advection equation

$$\frac{dC(\zeta)}{d\zeta} = \frac{\bar{\mu}_{net}(\zeta)}{w_s}C(\zeta) \quad (6)$$

where $\zeta = z + w_s t$. Assuming that growth rate can be represented by an average over time and space, the solution to Eq. 6 is Eq. 7.

$$C(z + w_s t, t) = C(z, 0)e^{\bar{\mu}_{net}t} \quad \text{for } z + w_s t < h \quad (7)$$

We refer to Eq. 7 as the linear model because the population is translated linearly down the water column at a constant rate over time τ_s. For a population initially uniformly
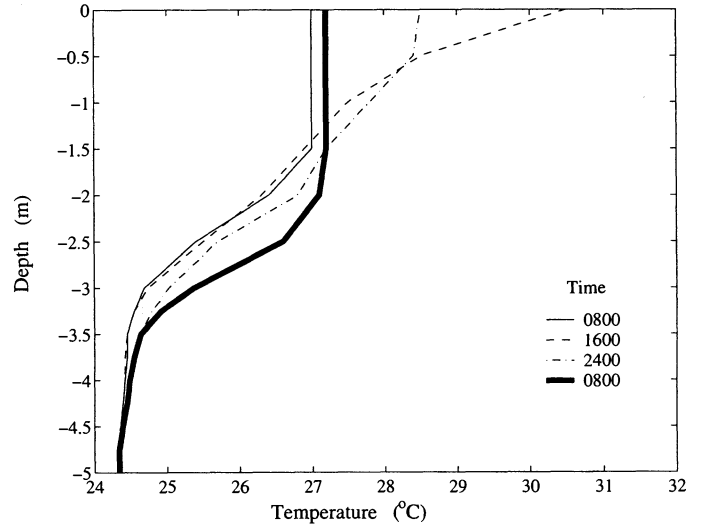

Fig. 1. Temperature profiles in Maude Weir Pool measured by thermistor chain TC-1 on 13–14 Jan 95 (adapted from Webster et al. 1996, *see* fig. 4.2).

distributed in the vertical, the depth-integrated concentration $C_z(t)$ for time $t < \tau_s$ is Eq. 8.

$$C_z(t) = \int_{w_s t}^{h} C(z + w_s t, t) \, dz$$

$$= \int_{0}^{h - w_s t} C(z, 0)e^{\bar{\mu}_{net}t} \, dz$$

$$= C_0\left(1 - \frac{t}{\tau_s}\right)e^{\bar{\mu}_{net}t} \quad (8)$$

Methods

Datasets—Two published datasets were used to examine the minimum mixing criteria for the growth of negatively buoyant phytoplankton. In the first of these datasets, temperature profiles and the depth-averaged concentration of *A. granulata* were measured over 0–5 m depth at Sta. TC-1 in Maude Weir Pool on the Murrumbidgee River in summer 1993–1994 and 1994–1995 (Webster et al. 1996; Sherman et al. 1998). Maximum daily mixing depth h_m was defined as the depth of well-mixed upper layers, as determined from the temperature profiles (Sherman et al. 1998). Under high flow conditions, the water column was continuously well mixed. Diurnal stratification developed under low flow, and nighttime cooling caused mixing to depth h_m, with vertical eddy diffusivity $K_z \sim 10^{-3}$–10^{-2} m² s⁻¹ (Bormans and Condie 1998). A typical diurnal cycle of temperature profiles is shown in Fig. 1, where $h_m = 1.5$ m. The mean daily photosynthetically active radiation (PAR) at position TVC-1 was $\bar{I}_0 = 11.7\varepsilon$ m⁻² d⁻¹, with light attenuation coefficient $\eta = 2.6$ m⁻¹ and $h \sim 5$ m (Sherman et al. 1998). For *A. granulata*, $w_s = 0.95$ m d⁻¹ (Sherman et al. 1998).

The second dataset was for the green alga *Scenedesmus* sp. Mesocosm experiments were conducted by Visser et al.

Table 2. Sediment trap data for *Scenedesmus* in mesocosm experiments (Visser et al. 1996*b*) and values of τ_s and w_s calculated by Eqs. 5 and 17.

	Experiment			
	Ia	Ib	IIa	IIb
Grazing	Yes	No	Yes	No
Mixing depth (m)	10	10	2	2
Net daily relative sedimentation (%)	7($\pm$4)	6($\pm$1)	27($\pm$15)	17($\pm$2)
Sedimentation time τ_s (d)	14	17	4	4
Sinking rate $w_s = h/\tau_s$ (m d^{-1})	0.7	0.6	0.5	0.5

(1996*b*) in two vertical columns, I and II, with constant mixing depths of 10 and 2 m, respectively (Table 2). The concentration of *Scenedesmus* cells in the top 2 m of Lake Nieuwe Meer over four summers (1990, 1991, 1993, 1994) was reported by Visser et al. (1996*a*), along with mixing depth calculated weekly from temperature profiles and wind data using the Wedderburn number (*see* Imberger and Hamblin 1982). *Scenedesmus* was considered to be uniformly distributed over the SML; hence, C_z in the SML was determined from h and the concentration in the top 2 m. Nutrients were present at saturation levels for *Scenedesmus* growth in the mesocosms and the lake, and the temperature was similar in each. During the periods of data collection in Lake Nieuwe Meer, the mean light attenuation coefficient was 1.2 ± 0.2 m^{-1}, and $\bar{I}_0 \sim 800$ $\mu\varepsilon$ m^{-2} s^{-1} (Visser et al. 1996*a*).

In 1993 and 1994 the lake was artificially destratified, increasing the SML depth in these years. Sedimentation data from the mesocosm experiments and Lake Nieuwe Meer (Tables 2, 3) are used to investigate the effect of mixing regime on sedimentation measurements.

Minimum mixing depth—Condie and Bormans (1997) proposed that negatively buoyant phytoplankton will not grow unless net growth exceeds sedimentation losses, and Huisman and Sommeijer (2002*b*) suggested that this condition corresponds to a minimum thermocline depth z_{Tmin}. This concept will be referred to hereafter as the minimum mixing depth h_{min}, because it incorporates both unstratified and stratified systems, so long as phytoplankton are not resuspended from the bottom boundary. The scale h_{min} can be determined by comparing the timescales for growth and sedimentation. The growth number G defines the relative magnitude of time scales for sedimentation and net growth (e.g., Koseff et al. 1993; Condie 1999).

$$G = \frac{\tau_s}{\tau_g} = \frac{\bar{\mu}_{net}(h)h}{w_s} \tag{9}$$

The relationship between h and G is nonlinear, since $\bar{\mu}_{net}$ is a nonlinear function of light availability and hence mixing depth h. To reflect this relationship, we define h_{min} as the minimum value of h for which $G > 1$, rather than use the equivalent definition of $z_{Tmin} = w_s/\bar{\mu}_{net}$ (Huisman and Sommeijer 2002*b*), where $\bar{\mu}_{net} = f(z_{Tmin})$. The vertical light gradient can be calculated from the Beer-Lambert equation

$$I(z,t) = I_0(t)e^{-\eta z} \tag{10}$$

where η is the light attenuation coefficient and $I_0(t)$ is the irradiance at the surface. Many different expressions have been published for light-limited growth of phytoplankton (e.g., Jassby and Platt 1976; McBride 1992). Because we are not considering photoinhibition, we have applied the Baly photosynthesis-irradiance model (Baly 1935), as used in many other modeling studies (e.g., Bormans and Condie 1998; Huisman et al. 1999, 2002*a*).

$$\mu_{net}(z, t) = \mu_{max}\frac{I(z, t)}{I(z, t) + I_k} \tag{11}$$

μ_{max} is the maximum growth rate (adjusted for respiration and grazing losses), $I(z, t)$ is the PAR at depth z and time t, and I_k is the half-saturation constant for irradiance.

For phytoplankton uniformly distributed in the vertical, the net depth-averaged daily growth can be calculated by integrating the net growth rate (Eq. 11) over depth.

$$\bar{\mu}_{net} = \frac{\mu_{max}}{\eta h}\ln\left(\frac{\frac{\bar{I}_0}{I_k} + 1}{\frac{\bar{I}_0}{I_k}e^{-\eta h} + 1}\right) \tag{12}$$

The net mean growth of *Scenedesmus* decreases linearly as $h:z_{eu}$ increases, where z_{eu} is the euphotic depth and $I_0 \sim 700$ $\mu\varepsilon$ m^{-2} s^{-1} (Ibelings et al. 1994). This relationship was used to solve for the minimum value of h for which $G > 1$

Table 3. Sediment trap data (SD) for *Scenedesmus* at $z_s = 20$ m in Lake Nieuwe Meer (Visser et al. 1996*a,b*) and with values of τ_s and w_s calculated by Eqs. 5 and 17.

	1990	1993	1994
Trap deployment period	12 Jul–30 Aug	22 Apr–26 Aug	18 May–30 Jun
SML depth h (m)	4(1)	23(4)	13(6)
Net daily sedimentation (%) (relative to biomass in SML)	36(11)	3(2)	9(2)
Sedimentation time τ_s (d)	3.5	40	11
Sinking rate w_s (m d^{-1})	1.2	0.6	1.2

Table 4. Phytoplankton characteristics and turbulent parameters typical of the surface mixing layer of lakes.

	Range	Source
Sinking rate w_s (m d^{-1})	10^{-3}–10^2	Reynolds et al. 1987
Mean net positive growth rate $\bar{\mu}_{net}$ (d^{-1})	0–5	Reynolds 1984
Surface mixing layer depth h (m)	1–100	
Vertical eddy diffusivity K_z (m^2 s^{-1})	10^{-3}–10^{-5}	MacIntyre 1993
Sedimentation time $\tau_s = h/w_s$ (d)	10^{-2}–10^5	
Growth number $G = \bar{\mu}_{net}h/w_s$	$<10^3$	Eq. 9
Peclet number Pe $= w_s h/K_z$	10^{-5}–10^4	Eq. 1

and, hence, to calculate h_{min} for *Scenedesmus* in Lake Nieuwe Meer.

In Maude Weir Pool under continuous mixing, substituting Eq. 12 into Eq. 9 yields the minimum value of h for which $G > 1$ (i.e., for which growth exceeds sedimentation losses). We used $\mu_{max} = 0.5$ d^{-1} and $I_k = 10$ $\mu\varepsilon$ m^{-2} s^{-1} for *A. granulata* (Bormans and Condie 1998), where μ_{max} was adjusted for respiration and grazing losses.

Because Maude Weir Pool alternated between continuous and diurnal mixing, h_{min} was calculated for both cases. To determine h_{min} in periods of diurnal mixing, we applied the linear model (Eq. 7) coupled to the growth and light equations (Eqs. 10, 11) during daylight hours, when the daily stratification cycle and values of K_z indicated that Pe $\gg$ 1. During the nighttime, when convective mixing occurred, Pe $\ll$ 1 for $z \leq h_m$, so the exponential model (Eq. 5) was applied with $G = 0$ in this region. The h_{min} was calculated by running the model for 5 d for increasing values of h_m, using increments of 10 cm. The minimum value of h_m for which growth occurred was defined as h_{min} for the diurnal system. The model was run with a time step of 18 min and 800 mesh points in the vertical.

Mixing and growth regimes—In order to define mixing and growth regimes, Eq. 2 was solved numerically for a range of values of Pe and G. In defining Pe, we accounted for the difference between the dispersion of tracers and phytoplankton in turbulence. Particle diffusivity in turbulence is modified by the crossing trajectories effect, by which dispersion is reduced as particles fall out of eddies because of gravity (Csanady 1963). Hence, the phytoplankton vertical eddy diffusivity K_{zp} will be lower than K_z for a tracer in the same flow (Csanady 1963), where $\beta = 0.356$ (Wang and Stock 1993).

$$\frac{K_{zp}}{K_z} = \left(1 + \frac{\beta^2 w_s^2}{w_{rms}^2}\right)^{-1/2} = (1 + \beta^2 Pe)^{-1/2} \qquad (13)$$

The reaction-advection-diffusion equation (Eq. 2) can be written as a function of G and Pe$_p = w_s h/K_{zp}$ using dimensionless depth and time variables (e.g., Koseff et al. 1993; Ruiz 1996). Hence, both Eq. 2 and the boundary conditions (Eq. 3) can be written directly in terms of G and Pe, since Pe$_p$ is a function of Pe (Eq. 13).

Equation 2 was solved with a third-order, upwind, implicit scheme. The "advection" and "diffusion" terms were implemented in two separate steps using the operator split approach (e.g., Clement et al. 1998). The grid step dz was defined by the distance fallen at sinking rate w_s in one time step, DT (i.e., Courant number $(w_s\,dt)/dz = 1$). This method resolved numerical diffusion issues that can arise with other numerical schemes. In each simulation, the population was initially uniform in the vertical, and Pe was constant and uniform.

To define mixing regimes, Eq. 2 was solved for $G = 0$ and 80 values of Pe in the range 10^{-4}–10^4 ($10^{-4} <$ Pe$_p <$ 10^7), the typical range of Pe in the SML of lakes (Table 4), The predictions of the exponential and linear equations (Eqs. 5, 7) were compared with the predictions of the full reaction-advection-diffusion equation. Because mixing affects total biomass $C_z(t)$ and vertical distribution $C(z, t)$, the models were compared using these two measures. As a measure of biomass, the retention time τ_n was defined as the time for normalized depth-integrated concentration $[C_z(t)/C_0]$ to decay to a given percentage, n.

To define growth regimes, Eq. 2 was solved over the range of Pe and G experienced by phytoplankton in the field (Table 4): $10^{-4} \leq$ Pe $\leq 10^4$ and $10^{-3} < G \leq 10^3$. For each value of Pe and G, the population was defined as "growing" if biomass had increased after time $10\tau_s$. This cutoff was chosen arbitrarily, and results were successfully replicated using both $8\tau_s$ and $15\tau_s$ as cutoff time.

Sedimentation—The vertical flux of phytoplankton cells into a sediment trap deployed at depth z_s will be a function of both w_s and $C(z, t)$ and, hence, will be affected by mixing regime. The sedimentation rate, SR, of a population with vertical distribution $C(z, t)$ is shown in Eq. 14.

$$SR(z_s, t) = w_s C(z_s, t) \qquad (14)$$

If Pe $\sim$ 1 or Pe $\gg$ 1, Eq. 2 or the linear model (Eq. 7) must be solved for $C(z_s, t)$, and sedimentation rate will vary over depth and time, as we will show later. However, if Pe $\ll$ 1, the exponential model (Eq. 5) can be substituted into Eq. 14, and SR is written in terms of G and τ_s.

$$SR(z_s, t) = \frac{w_s}{h}C_z(t) = \frac{1}{\tau_s}C_0 e^{(G-1)(t/\tau_s)} \qquad (15)$$

The net sedimentation $NS(z_s, t)$ is the total mass deposited at depth z_s over time t. For Pe $\ll$ 1, net sedimentation NS can be written as in Eq. 16.

$$NS(t) = \int_0^t \frac{1}{\tau_s}C_0 e^{(G-1)(t/\tau_s)}\,dt$$

$$= \frac{1}{G-1}C_0[e^{(G-1)(t/\tau_s)} - 1] \qquad (16)$$

Because NS depends on the magnitude of the overlying biomass, it is often normalized by $C_z(t)$ to define the relative net sedimentation, RNS. For Pe $\ll$ 1, RNS can be written from Eqs. 5, 9, and 16 as Eq. 17.

$$\text{RNS}(t) = \frac{\text{NS}(t)}{C_z(t)} = \frac{1}{G-1}[1 - e^{-(G-1)(t/\tau_s)}] \qquad (17)$$

We estimated $(G-1)/\tau_s$ for *Scenedesmus* in the mesocosm experiments and in Lake Nieuwe Meer by applying Eq. 5 to the published plots of depth-averaged concentration over time (Visser et al. 1996*a,b*). By substituting $(G-1)/\tau_s$ into Eq. 17 with the sediment trap data (Visser et al. 1996*b*), we calculated G, τ_s, and hence w_s (Table 2).

Net daily relative sedimentation measurements of *Scenedesmus* varied widely between years in Lake Nieuwe Meer and between the lake and the mesocosm experiments (Table 2). We applied a simple two-layer model (as per Condie and Bormans 1997) to determine whether these variations could be explained by differences in mixing regimes.

In 1990 and 1994, mean SML depth was less than the trap deployment depth $z_s = 20$ m. The exponential model (Eq. 5) was applied for $z \leq h$, and the linear model (Eq. 7) was applied for $h < z \leq z_s$ to determine vertical distribution $C(z, t)$. The population was treated as initially uniform in the vertical, with $w_s = 0.6$ m d^{-1}. The net daily sedimentation was calculated by integrating Eq. 14 over 24 h. For comparison with the sediment trap data reported by Visser et al. (1996*b*), relative daily sedimentation was defined as the ratio of net daily sedimentation to the depth-integrated concentrations in the surface mixing layer.

Results

In Maude Weir, $h_{min} = 2.7$ m was predicted for *A. granulata* under diurnal mixing conditions and $h_{min} = 1.4$ m during continuous mixing. Depth-averaged concentration of *A. granulata* and the maximum daily mixing depth h_m are plotted against time in Fig. 2. Periods of continuous mixing, when the pool was isothermal for the entire day, were distinguished from periods of diurnal mixing by the minimum temperature difference over the water column (Sherman et al. 1998), and the values of h_{min} are plotted in Fig. 2 accordingly.

During periods of diurnal mixing, the *A. granulata* population did not grow unless $h_m \geq 2.5$ m (Fig. 2). During periods of continuous mixing, caused by high river flow, growth occurred for $h > h_{min} = 1.4$ m, but we could not assess the system for $h < h_{min}$ because the entire water column was mixed ($h = 5$ m). Furthermore, the population might have been affected by horizontal advection during this time. Hence, we were not able to validate the magnitude of h_{min} predicted for continuous mixing.

In Lake Nieuwe Meer, $h_{min} = 3.2 \pm 0.3$ m was predicted for *Scenedesmus*. The depth-integrated concentration and mixing depth are plotted against time in Fig. 3. In 1990 and 1991, net growth occurred generally when the SML was deeper than 6 m (Fig. 3a,b). The relationship between mixing depth and *Scenedesmus* biomass was not as strong in 1993 and 1994 (Fig. 3c,d), although population decay still oc-
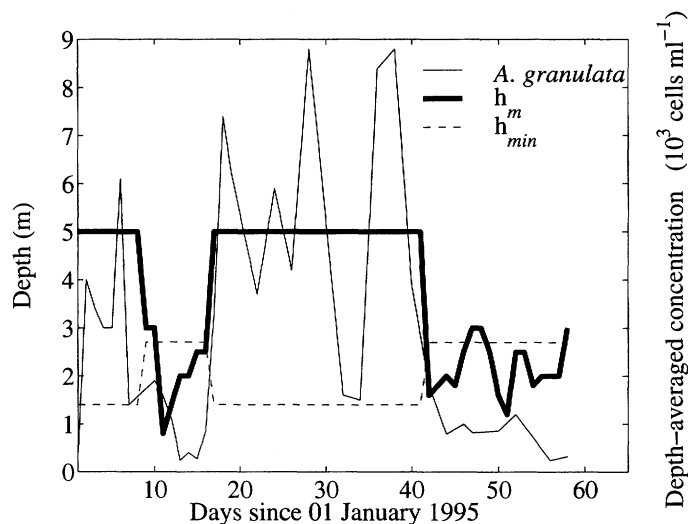

Fig. 2. Measured maximum daily mixing depth, h_m, and depth-averaged concentration of *A. granulata* plotted against time for Maude Weir Pool (Sherman et al. 1998). Model predictions give $h_{min} = 2.7$ m during diurnal mixing and $h_{min} = 1.4$ during continuous mixing.

curred when surface mixing depth was, occasionally, less than ~6 m. Under these conditions, $h_{min} \sim 6$ m. Both the predicted and the observed values of h_{min} (3.2 and 6 m, respectively) are plotted in Fig. 3.

From simulations with the reaction-advection-diffusion equation (Eq. 2) for $G = 0$, it can be concluded that for Pe ≤ 0.1, the exponential model provides accurate predictions of phytoplankton or particle retention time. This can be seen by comparing the values of τ_{37}, τ_{10}, and τ_{01} calculated from the numerical solution of Eq. 2 (Fig. 4) with the values calculated from the exponential model (Table 5). For Pe ≤ 0.1, the vertical profile is uniform, as predicted by the exponential model (Fig. 5a,b). For Pe ≥ 100, the linear model provides good predictions of both the retention time (Fig. 4; Table 5) and the vertical profile (Fig. 5e,f). For $0.1 < \text{Pe} < 100$, the full reaction-advection-diffusion equation must be used in conjunction with the "crossing trajectory" correction for K_{zp} (Eqs. 2, 13) to predict either vertical distribution $C(z, t)$ or depth-integrated concentration $C_z(t)$.

From the solution of Eq. 2 for $G > 0$, the regions of growth and decay were defined in terms of Pe and G. Each of the three mixing regimes defined above is made up of two growth regimes, as shown in Fig. 6.

For Pe ≤ 0.1, the population will be uniformly distributed in the vertical (Fig. 5), consistent with the laboratory results of Webster and Hutchinson (1994), unless $\tau_g/\tau_{mix} \ll 1$. The exponential model (Eq. 5) can be written in terms of G and τ_s to show that the characteristic timescale τ_c for the population is $\tau_s/(G-1)$. Hence, if $G < 1$, $\tau_c < 0$ and the population decays over time (growth regime A in Fig. 6; Table 6). If $G > 1$, $\tau_c > 0$ and the population grows (regime B). For very rapid growth at very slow sinking rates, $G \gg 1$ and the population grows exponentially with timescale $\tau_c = \tau_g$, consistent with growth models that neglect sedimentation (e.g., Reynolds 1984). As G approaches unity, the population reaches steady state. In the mesocosm experiments of Visser
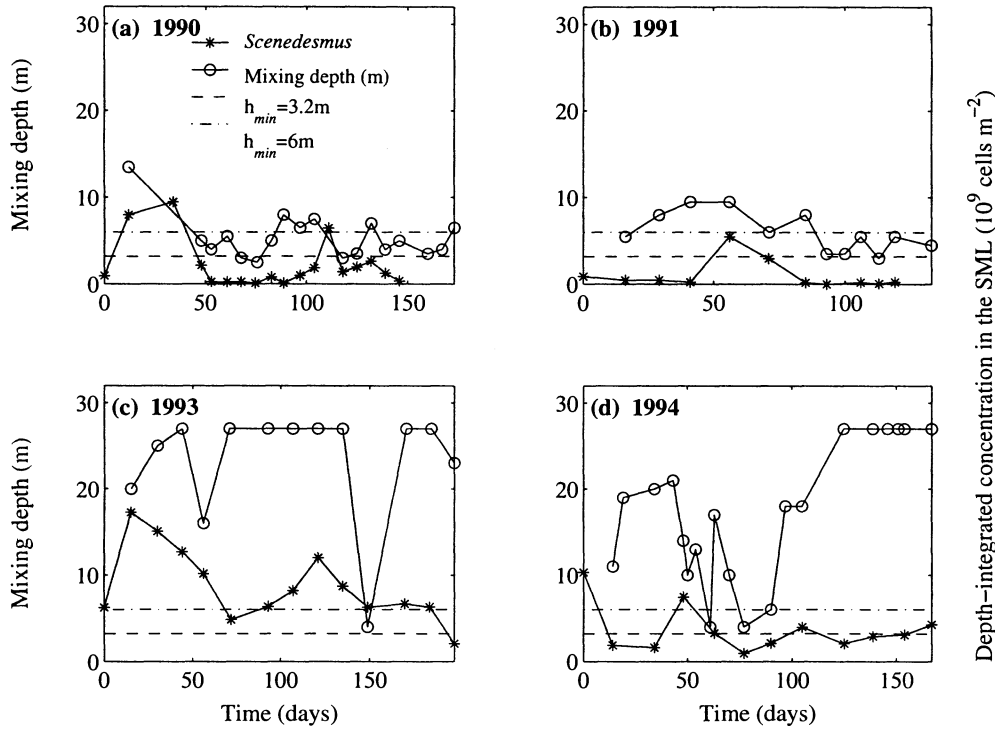
Fig. 3. Predicted surface mixing layer depth, *h,* and measured depth-integrated concentration, C_z, of *Scenedesmus* sp. in Lake Nieuwe Meer (Visser et al. 1996*a*) plotted against time for 4 yr: (a) from 16 Mar 90, mean mixing depth $\bar{h}$ = 6 m (SD = 3 m); (b) from 24 Apr 91, $\bar{h}$ = 6 m (SD = 2 m); (c) from 23 Mar 93, $\bar{h}$ = 23 m (SD = 7 m); (d) from 14 Apr 94, $\bar{h}$ = 17 m (SD = 8 m). Model predictions give h_{min} = 3.2 m, but observation suggests h_{min} = 6 m.
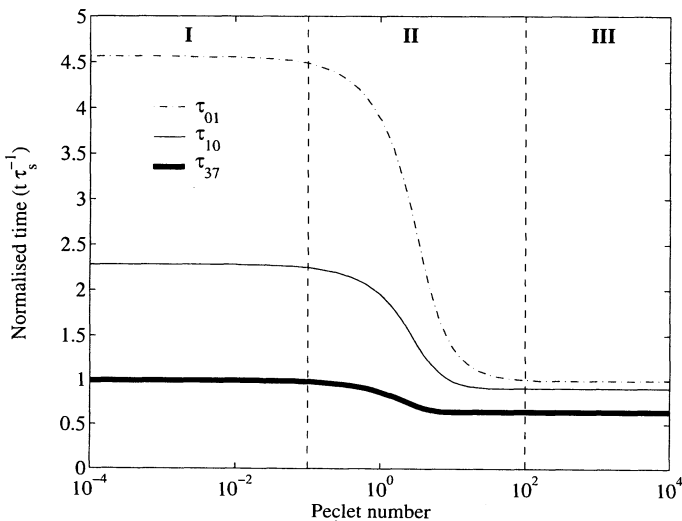

Fig. 4. Phytoplankton retention time predicted by Eq. 2 (with crossing trajectory correction) for an initially uniform vertical distribution of phytoplankton and $G \ll 1$, sinking at rate w_s in a SML of depth h. τ_n is the time for normalized depth-integrated concentration, C_z/C_0, to reach n%. Three mixing regimes are shown, characterized by different models for τ_n: (I) exponential model, (II) reaction-advection-diffusion equation, and (III) linear model (*see* Table 5).

et al. (1996*b*), *Scenedesmus* lay in the population decay regime A, when grazers were present in high concentrations, and in growth regime B, when grazers were removed.

If Pe $\geq$ 100, the phytoplankton distribution can be described by the linear equation (Eq. 7). Under these conditions, the entire phytoplankton population will sink out of the SML by time τ_s, regardless of the value of *G.* By taking the derivative of C_z with respect to time, it can be shown that if $G \leq 1$, the total biomass will decay monotonically over time ($dC_z/dt < 0$, growth regime E in Fig. 6, Table 6). If $G > 1$, however, the biomass will increase initially before decaying by time τ_s (regime F). In the case of intermittent

Table 5. Retention time calculated for a phytoplankton population, initially uniform in the vertical, and sinking at rate w_s in a mixing layer of depth h, for $G \ll 1$. The time for normalized depth-integrated concentration $C_z(t)/C_0$ to reduce to 1, 10, and 37% is calculated as a fraction of sedimentation time τ_s. The exponential model (Eq. 5) describes the case where Pe $\ll$ 1, and the linear model (Eq. 7) describes the case where $Pe_p \gg 1$.

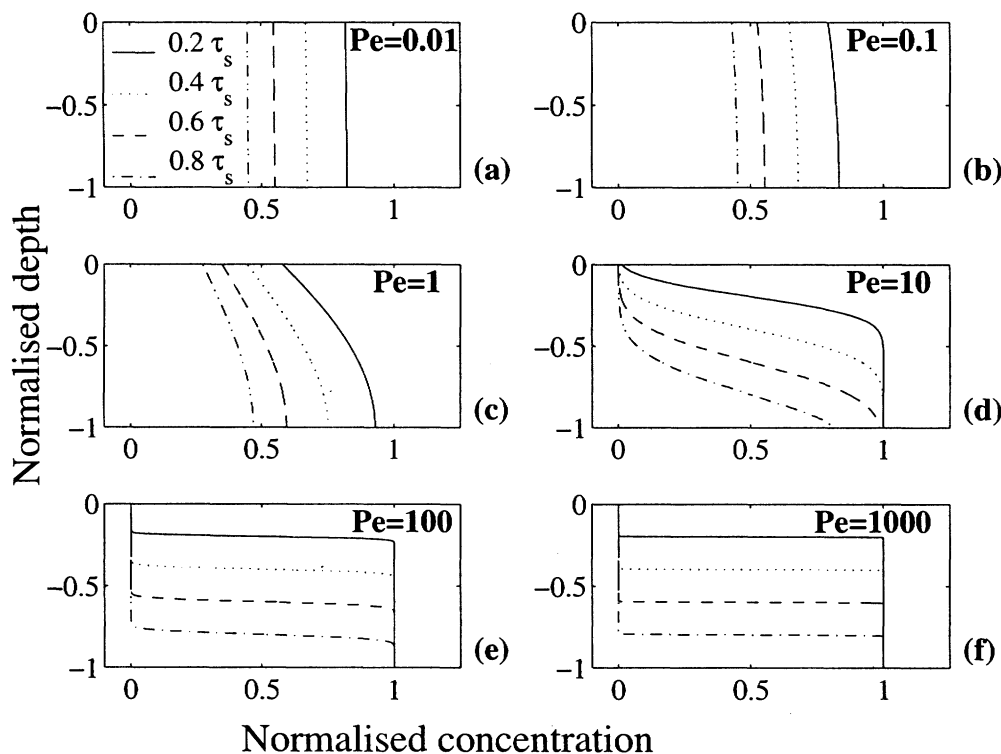|	Retention (%)	Exponential model	Linear Model
τ_{01}	1	$4.6\tau_s$	$0.99\tau_s$
τ_{10}	10	$2.3\tau_s$	$0.90\tau_s$
τ_{37}	37	$1.0\tau_s$	$0.63\tau_s$
τ_n	n	$\ln(100/n)\,\tau_s$	$[1 - (n/100)]\,\tau_s$

Fig. 5. Normalized vertical profiles $[C(z, t)]/[C(z, 0)]$, predicted by the reaction-advection-diffusion equation (with crossing trajectory correction) for an initially uniform vertical distribution of phytoplankton and $G \ll 1$, sinking at rate w_s in a SML of depth h. The profiles are plotted over normalized depth (z/h) at four time steps—$0.2\tau_s$, $0.4\tau_s$, $0.6\tau_s$, and $0.8\tau_s$—for six values of the Peclet number: (a) Pe = 0.01, (b) Pe = 0.1, (c) Pe = 1, (d) Pe = 10, (e) Pe = 100, (f) Pe = 1,000. The solution moves from small Pe (a, b), where it is well described by the exponential model, to large Pe in (e, f), where the profile is consistent with the linear model.

stratification for periods less than τ_s, population growth is more likely in regime F than in regime E.

No simplifications of Eq. 2 are possible when $0.1 <$ Pe < 100. In general terms, growth occurs when G is large and Pe small (growth regime D in Fig. 6, Table 6). If the value of G relative to Pe is not high enough, the phytoplankton population will lie in regime C and decay over time. The curve dividing these two regions was derived directly from the solution of the reaction-advection-diffusion equation. For Pe > 1, the crossing trajectory effect becomes significant; K_z should be replaced by K_{zp}, calculated from Eq. 13, and Pe should be recalculated from Eq. 1 using K_{zp}.

From the mesocosm experiments with *Scenedesmus* and Eq. 17, we calculated $w_s = 0.6 \pm$ m d^{-1} (Table 2). In 1993, the sediment trap in Lake Nieuwe Meer was deployed consistently below the SML depth, and the sinking rate $w_s = 0.6$ m d^{-1} was calculated from Eq. 17. In 1990 and 1994, however, mean SML depth was significantly less than the sediment trap deployment depth, $z_s = 20$ m. Under these conditions, it was not valid to assume that Pe ≤ 0.1 above the trap. Net daily relative sedimentation in these 2 yr was predicted from the two-layer model as discussed earlier, and these results are shown in Fig. 7. These predictions are of comparable magnitude to the measured values in Table 2, whereas Eq. 17 resulted in consistent underprediction.

Discussion

If the SML is too shallow ($h < h_{min}$), sedimentation losses exceed growth and phytoplankton populations decay over time. This hypothesis of Huisman and Sommeijer (2002b) is shown here to be supported by the two datasets: growth of *A. granulata* in Maude Weir Pool and *Scenedesmus* in Lake Nieuwe Meer were restricted by sedimentation losses when $h < h_{min}$. The predicted value of $h_{min} = 2.7$ m for *A. granulata* during diurnal mixing showed good agreement with field data, but $h_{min} = 3.2$ m predicted for *Scenedesmus* was approximately half of the observed value of 6 m. This difference could have been due to restriction of *Scenedesmus* growth in Lake Nieuwe Meer by grazing ($\bar{\mu}_{net}$ determined by Ibelings et al. [1994] did not include grazing) or to overestimation of the *Scenedesmus* growth rate arising from the use of a daily average irradiance in the model (cf. McBride 1992; Wallace et al. 1996).

The minimum mixing depth, h_{min}, can be estimated from time series of mixing depth and phytoplankton biomass, as shown for Lake Nieuwe Meer. This means that h_{min} can be determined for a given species in a given system without any modeling and, thus, used in conjunction with measurement or prediction of h as a simple management tool to predict whether the phytoplankton will grow or decay over
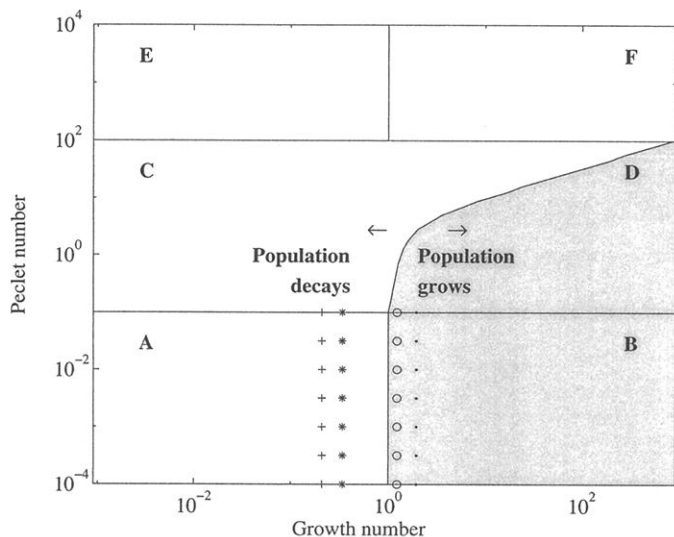
Fig. 6. Growth regimes predicted by the reaction-advection-diffusion equation (with crossing trajectory correction) for phytoplankton initially uniform in the vertical, sinking at rate w_s in a SML of depth h. The shaded region of the plot indicates where phytoplankton populations will grow over time. In the unshaded regions, populations will decay. Six growth regimes are defined: (A) population decays exponentially over time, (B) population grows exponentially, (C, D) as Pe increases, a larger value of G is necessary for the population to grow, (E) population decays monotonically over time, and (F) biomass increases initially, but decays completely by time τ_s. Mesocosm data from Visser et al. (1996*b*) is also plotted: (+) Ia, (○) Ib, (asterisk) IIa, (●) IIb (*see Table 2*).
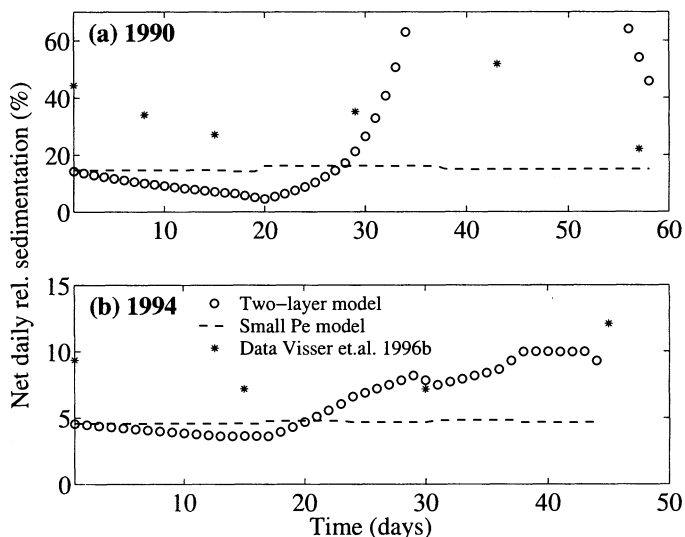

Fig. 7. Measured and predicted values of net daily relative sedimentation of *Scenedesmus* at $z_s = 20$ m in Lake Nieuwe Meer (Eq. 14). The two-layer model uses Pe ≤ 0.1 in the surface mixing layer and Pe ≥ 100 below. The small Pe model uses Eq. 15. Both models use $w_s = 0.6$ m d^{-1}, with G and h calculated from the field data of Visser et al. (1996*b*). (a) 1990, (b) 1994.

time. Although G can also be used to predict phytoplankton population dynamics (Condie and Bormans 1997), it includes a measure of growth, which requires modeling or more extensive field data than simply measuring or estimating h.

The magnitude of G, and hence h_{min}, can be affected by either the light-harvesting efficiency of a given species, or the light conditions to which it is exposed (i.e., I_0 and η). An example of the latter is the change in mixing regime in Maude Weir Pool, which caused a difference by a factor of two in the h_{min} predicted for *A. granulata*. Continuous mixing allows negatively buoyant phytoplankton to be maintained higher in the water column and receive a higher photon dose than under stratified conditions; hence, less mixing is required to overcome sedimentation losses.

The general relationship between light availability and mixing depth in the absence of photoinhibition is illustrated in Fig. 8 for three specific sets of light and growth conditions. The curves show how higher growth rates lead to reduced h_{min} because less mixing is required to obtain net growth and overcome sedimentation losses. They also demonstrate that if growth conditions are adverse, no value of h_{min} exists, and the population will not grow for any value of mixing depth. Photoinhibition has been observed to restrict growth in reservoirs if mixing is too shallow (Grobbelaar 1990). In Maude Weir, the high turbidity and, in the case of diurnal mixing, low residence time of phytoplankton near the surface, mean that photoinhibition is unlikely to affect growth (cf. Kirk 1994). *Scenedesmus* is also almost certainly not affected by photoinhibition for the values of incident irradiance and surface mixing depth measured in Lake Nieuwe Meer (Ibelings et al. 1994). Although photoinhibition did not play an important role in either of the datasets considered here, it might be significant in other systems, and so should be considered in any models predicting h_{min}.

The relationship between h_{min} and Sverdrup's critical depth is illustrated in Fig. 8 for a surface mixing layer where Pe ≤ 0.1. The Sverdrup depth represents a balance between mixing, growth, and respiration; hence it is defined by the point where $\mu_{net} = 0$ (Sverdrup 1953). The balance between

Table 6. Summary of growth regimes, including timescales and dynamics.

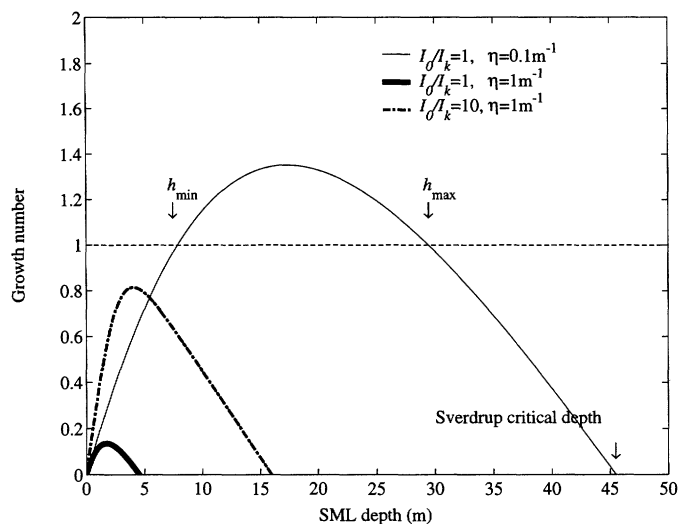| Regime	Pe	G	Dynamics	Timescale
A	Pe≤ 0.1	$G<1$	Exponential decay	$\tau_c = \tau_s/(G-1)$
B	Pe≤ 0.1	$G>1$	Exponential growth	$\tau_c = \tau_s/(G-1)$
C	$0.1<$Pe<100	$G<$critical function	Decay	
D	$0.1<$Pe<100	$G>$critical function	Growth	
E	Pe≥ 100	$G\leq 1$	Monotonic decay	$\tau_c = \tau_s$
F	Pe≥ 100	$G>1$	Initial increase, then decay	$\tau_c = \tau_s$

Fig. 8. Growth number, $G = \bar{\mu}_{net}h/w_s$, plotted against surface mixing layer (SML) depth. Depth-averaged net growth, $\bar{\mu}_{net}$, is calculated from Eq. 12 for three examples of light attenuation η and irradiance ratio $\bar{I}_0/I_k$ assuming $\mu_{max}/w_s = 0.5 \text{ m}^{-1}$ (e.g., *A. granulata*), respiration = 10% of μ, and grazing = 5% of μ. The figure illustrates the general relationship between growth and sinking conditions, and h_{min} and the Sverdrup depth. For a species with higher μ_{net}/w_s or in a system with higher incident irradiance or lower light attenuation, h_{min} would be less and the Sverdrup depth greater than shown here.

mixing, net growth, and sedimentation, however, is defined by the condition $G > 1$, and both a minimum h_{min} and a maximum h_{max} mixing depth might exist for net population growth. This is consistent with the nonmonotonic relationship between mixing depth and phytoplankton growth proposed in estuaries (Lucas et al. 1998) and with model results of Huisman and Sommeijer (2002*b*) for turbulent eddy diffusivity greater than some critical value for a given set of sedimentation and growth parameters. When sedimentation losses are important, the Sverdrup critical depth could significantly overestimate the maximum mixing depth at which the population can be sustained, as for example, in Fig. 8.

The exponential and linear models (Eqs. 5, 7) derived from Eq. 2 indicate that the vertical distribution of phytoplankton and their retention and growth times are independent of K_z for Pe ≤ 0.1 and Pe ≥ 100. Hence, variations in vertical eddy diffusivity K_z over time or space will only affect the biomass or distribution of a phytoplankton population if $0.1 < $ Pe < 100 or if there are changes in mixing regime. Hence, although K_z decays over depth in the case of wind mixing (e.g., Yamazaki and Kamykowski 1991), this variation will not necessarily influence vertical distribution or total phytoplankton biomass in the SML.

It has often been suggested that turbulence dominates phytoplankton populations if Pe $\ll 1$ and that sedimentation dominates for Pe $\gg 1$ (e.g., Humphries and Lyne 1988; MacIntyre 1989; Pesant et al. 2002). Although turbulence homogenizes the vertical profiles of phytoplankton for Pe ≤ 0.1, it is clear from our simulations and the published data from Lake Nieuwe Meer and Maude Weir that population growth in this mixing regime can still be dominated by sed-

imentation if $G < 1$ (Fig. 6). For $G \ll 1$, the population decays exponentially with timescale $\tau_c \sim -\tau_s$, consistent with models of sedimentation for passive particles such as sediments, fecal pellets, or marine snow (Smith 1982; Martin and Nokes 1988).

Mixing and growth regimes have been defined here in terms of a single value of Pe and G, but in practice, Pe and hence mixing regime can vary over space and time. These variations can often be accounted for by coupling the exponential and linear models, as we have shown. Over short times ($t \ll \tau_s$), the exponential model also can be approximated by the linear model (e.g., Thomas and Finney 1988). Hence, in a well-mixed system (Pe ≤ 0.1), temporary variations in mixing regime will not affect population dynamics if they occur over timescales that are small compared to the sedimentation time. When the period of stratification is small compared to τ_s, these diurnal systems can be treated as continuously mixed, greatly simplifying any predictive models.

The regimes defined in Fig. 6 can be used to predict the effect of changes in mixing or growth conditions on phytoplankton population dynamics. For example, in the second set of mesocosm experiments (Visser et al. 1996*b*), a decrease in grazing led to an increase in $\bar{\mu}_{net}$ and hence in G. This corresponded to a change in growth regime from A to B (Table 6) (i.e., from a regime in which the population decayed to one in which it grew). However, altering the turbulence intensity in the mesocosms would not affect these experiments unless Pe were increased to >0.1. Thus, we have provided a useful framework for assessing how various changes in, for example, turbidity or mixing in a water body can affect phytoplankton species composition and biomass. For a meaningful analysis of population dynamics, rate of population growth or decay must be defined, as well as regions where growth is possible (Smetacek and Passow 1990), as in Table 6.

Some of the advantages of the nondimensional approach can be seen by comparing Fig. 6 with the dimensional regime plots of Huisman et al. (1999, 2002*a*) and Huisman and Sommeijer (2002*b*). First, Fig. 6 is not restricted to a sedimentation and growth parameters of a particular species. Furthermore, it is not restricted to specific light, nutrient, or grazing conditions. For example, Huisman and Sommeijer (2002*b*) used two separate growth regimes in Fig. 6 in their paper to define when the surface mixing layer is either too shallow or too deep, respectively, to sustain a population in a highly turbulent environment. Both cases are incorporated in growth regime A in Fig. 6: Pe ≤ 0.1, $G < 1$. A population can also be restricted to region A for intermediate values of h because of grazing losses, nutrient limitation, and so on. Where two general formats for dimensional regime diagrams were defined for "high" and "low to moderate" values of w_s (Ebert et al. 2001; Huisman et al. 2002*a*), we have defined a single plot by using the Peclet number rather than individual variables.

The simple approach used in this paper relies on a number of assumptions. In determining growth and mixing regimes, constant and uniform values of $\bar{\mu}_{net}$, and hence G, were assumed. A regime with Pe ≤ 0.1 implies that the phytoplankton are uniformly distributed, which will not be true if $\tau_g/\tau_{mix} \ll 1$. However, because $\tau_g/\tau_{mix} = 1/(G \cdot \text{Pe})$, a situation

where Pe ≤ 0.1 and $\tau_g/\tau_{mix} \ll 1$ will only occur simultaneously for $G > 100$. Thus, our analysis excludes neutrally buoyant phytoplankton, for example ($w_s = 0$, G undefined). Even for very fast growing species ($\bar{\mu}_{net} = 1$ m d^{-1}), our assumptions are still valid for $w_s > 0.1$ m d^{-1}, and for slower growth rates, lower sinking rates will be valid. For Pe ≥ 100, G will only be constant for optically shallow waters; hence, Eq. 8 will only be valid for shallow, low-turbidity systems. Although the assumption of depth-invariant G has these limitations, the mixing regimes provide a clear indication of where the depth-dependent growth equations (Eqs. 10, 11) can be coupled with the advection equation (Eq. 7) or the full reaction-advection-diffusion equation (Eq. 2) to accurately describe both biomass and vertical distribution.

The boundary conditions used here rely on the assumption that K_{zp} approaches zero at the bottom boundary and that phytoplankton that reach the bottom of the water column will not be resuspended. These boundary conditions might not be valid where strong currents occur along the bed, and results are not directly applicable to positively buoyant particles, where surface scums and re-entrainment must be considered. Phytoplankton sinking rates have been assumed to be constant, but our results can be adapted for cases where w_s changes over depth and time because of nutrient availability or aggregation (e.g., Smayda 1970; Lande and Wood 1987; Waite and Nodder 2001). Although aggregation has a large effect on total sediment fluxes in the deep surface mixing layers of the open ocean, where the sedimentation time of individual phytoplankton is long (e.g., Hill 1992) it is not as important in sediment fluxes of the shallower systems considered here.

Mixing regimes have a large effect on the vertical profile of phytoplankton populations (Ruiz et al. 1996; Condie 1999) and, hence, on sediment trap results, as can be seen from the Lake Nieuwe Meer data. In 1990 and 1994, SML depth in the lake was much less than the trap deployment depth of $z_s = 20$ m. *Scenedesmus* sinking rate calculated from the trap data was overestimated by a factor of two by Visser et al. (1996*b*) when using the small Pe approximation (Eq. 17) in 1990 and 1994 (Tables 2, 3). When the two-layer model was applied to the lake using the sinking rate calculated from the mesocosm experiments ($w_s = 0.6$ m d^{-1}), predictions of net daily sedimentation were comparable to the sediment trap measurements (Fig. 7). This indicated that the sinking rate $w_s = 0.6$ m d^{-1} was consistent with the 1990 and 1994 sediment trap data if allowance was made for the mixing regimes above the trap. These results also illustrate that failure to quantify mixing regimes as a part of sediment trap analysis can lead to large errors. In relatively shallow systems such as lakes, where w_s is approximately constant for many negatively buoyant phytoplankton species, placing the trap above or close to the thermocline will allow the exponential model (Eq. 17) to be applied, greatly simplifying interpretation of the data.

Ruiz (1996) acknowledged that the simplified sedimentation models (Eqs. 15–17) are only applicable for Pe < 1. He attempted to develop a general equation for sedimentation, valid for all values of Pe, by introducing a linear correction factor F into Eq. 15, where F $= [hC(h, t)]/[C_z(t)]$. Although this model introduces great simplicity to sedimen-

tation models, we argue that it cannot be practically applied. The value of F reached an asymptotic value for $t > 2\tau_s$ when the vertical profile was considered to have reached a constant shape (Ruiz 1996). For Pe > 1, however, $<10\%$ of the initial population will remain in the system by time $2\tau_s$ (Fig. 4); a sedimentation model that is only valid for Pe > 1 after this time will not capture the bulk of the sedimentation. By contrast, the coupled linear-exponential models used here are valid for all time.

This study shows that it is the relative rather than absolute rates of mixing, growth, and sedimentation that control the growth of negatively buoyant phytoplankton populations. We are able to use the two dimensionless parameters, Pe and G, to describe the effects of mixing, growth, and sedimentation on different phytoplankton populations and to indicate how these parameters have general applicability to growth regimes. These parameters are not confined to a particular study in a specific system but have potential application in different lakes, reservoirs, and river pools for negatively buoyant phytoplankton where the growth time is not significantly less than the mixing time. By quantifying a change in an aquatic system in terms of Pe and G, the effect on a given species can be estimated from the change, if any, in growth or mixing regime. Our findings are particularly relevant to cases where SML is too shallow, as defined by h_{min} (Huisman and Sommeijer 2002*b*), and sedimentation losses restrict phytoplankton growth even if Pe $\ll 1$.

The mixing regimes defined in this paper have two important applications. First, these regimes define when simplified analytical models can be used in place of the full reaction-advection-diffusion equation to predict the vertical distribution and biomass of phytoplankton populations. Second, we have used these regimes to provide a simple framework for interpreting sediment trap data. Failure to account for water column mixing regime can lead to significant errors in estimates of sedimentation, as we have shown in Lake Nieuwe Meer. This work could be further extended to consider positively buoyant phytoplankton, such as cyanobacteria, by incorporating in the model the re-entrainment of phytoplankton from the surface.

References

BALY, E. C. 1935. The kinetics of photosynthesis. Proc. R. Soc. Lond. Ser. B **117:** 218–239.

BORMANS, M., AND S. A. CONDIE. 1998. Modelling the distribution of *Anabaena* and *Melosira* in a stratified river weir pool. Hydrobiologia **364:** 3–13.

CLEMENT, T. P., Y. SUN, B. S. HOOKER, AND J. N. PETERSEN. 1998. Modeling multispecies reactive transport in ground water aquifers. Ground Water Monitoring Remediation J. **18:** 79–92.

CONDIE, S. A. 1999. Settling regimes for non-motile particles in stratified waters. Deep-Sea Res. I. **46:** 681–699.

———, AND M. BORMANS. 1997. The influence of density stratification on particle settling, dispersion and population growth. J. Theor. Biol. **187:** 65–75.

CSANADY, G. T. 1963. Turbulent diffusion of heavy particles in the atmosphere. J. Atmos. Sci. **20:** 201–208.

EBERT, U., M. ARRAYAS, N. TEMME, B. SOMMEIJER, AND J. HUISMAN. 2001. Critical conditions for phytoplankton blooms. Bull. Math. Biol. **63:** 1095–1124.

GROBBELAAR, J. U. 1990. Modelling phytoplankton productivity in

turbid waters with small euphotic to mixing depth ratios. J. Plankton Res. **12:** 923–931.

HILL, P. S. 1992. Reconciling aggregation theory with observed vertical fluxes following phytoplankton blooms. J. Geophys. Res. **97**(C2): 2295–2308.

HUISMAN, J., P. VAN OOSTVEEN, AND F. J. WEISSING. 1999. Critical depth and critical turbulence: Two different mechanisms for the development of phytoplankton blooms. Limnol. Oceanogr. **44:** 1781–1787.

———, M. ARRAYÁS, U. EBERT, AND B. SOMMEIJER. 2002*a*. How do sinking phytoplankton species manage to persist? Am. Nat. **159:** 245–254.

———, AND B. Sommeijer. 2002*b*. Population dynamics of sinking phytoplankton in light-limited environments: Simulation techniques and critical parameters. J. Sea. Res. **48:** 83–96.

HUMPHRIES, S. E., AND V. D. LYNE. 1988. Cyanophyte blooms: The role of cell buoyancy. Limnol. Oceanogr. **33:** 79–91.

IBELINGS, B. W., B. M. KROON, AND L. R. MUR. 1994. Acclimation of photosystem II in a cyanobacterium and a eukaryotic green alga to high and fluctuating photosynthetic photon flux densities, simulating light regimes induced by mixing in lakes. New Phytol. **128:** 407–424.

IMBERGER, J., AND P. F. HAMBLIN. 1982. Dynamics of lakes, reservoirs and cooling ponds. Ann. Rev. Fluid Mech., **14:** 153–187.

JASSBY, A. D., AND T. PLATT. 1976. Mathematical formulation of the relationship between photosynthesis and light for phytoplankton. Limnol. Oceanogr. **21:** 540–547.

KIRK, J. T. 1994. Light and photosynthesis in aquatic ecosystems, 2nd ed. Cambridge Univ. Press.

KOSEFF, J. R., J. K. HOLEN, S. G. MONISMITH, AND J. E. CLOERN. 1993. Coupled effects of vertical mixing and benthic grazing on phytoplankton populations in shallow, turbid estuaries. J. Mar. Res. **51:** 843–868.

LANDE, R., AND A. M. WOOD. 1987. Suspension times of particles in the upper ocean. Deep-Sea Res. **34:** 61–72.

LUCAS, L. V., J. E. CLERN, J. R. KOSEFF, S. G. MONISMITH, AND J. K. THOMPSON. 1998. Does the Sverdrup critical depth model explain bloom dynamics in estuaries? J. Mar. Res. **56:** 375–415.

MACINTYRE, S. 1993. Vertical mixing in a shallow, eutrophic lake: Possible consequences for the light climate of phytoplankton. Limnol. Oceanogr. **38:** 798–817.

———. 1998. Turbulent mixing and resource supply to phytoplankton, p. 561–590. *In* J. Imberger [ed.], Physical processes in lakes and oceans. American Geophysical Union.

MARTIN, D., AND R. NOKES. 1988. Crystal settling in a vigorously convecting magma chamber. Nature **332:** 534–536.

MCBRIDE, G. B. 1992. Simple calculation of daily photosynthesis by means of five photosynthesis-light equations. Limnol. Oceanogr. **37:** 1796–1808.

OKUBO, A. 1980. Diffusion and ecological problems: Mathematical models. Springer-Verlag.

PESANT, S., L. LEGENDRE, M. GOSSELIN, E. BAUERFEIND, AND G. BUDEUS. 2002. Wind triggered events of phytoplankton downward flux in the Northeast Water Polynya. J. Mar. Sys. **31:** 261–278.

REYNOLDS, C. S. 1984. The ecology of freshwater phytoplankton. Cambridge Univ. Press.

———. 1998. Plants in motion: Physical-biological interaction in the plankton, p. 535–560. *In* J. Imberger [ed.], Physical processes in lakes and oceans. American Geophysical Union.

———, R. L. OLIVER, AND A. E. WALSBY. 1987. Cyanobacterial dominance: The role of buoyancy regulation in dynamic lake environments. New Zealand J. Mar. Fresh. Res. **21:** 379–390.

RIEBESELL, U. 1989. Comparison of sinking and sedimentation rate measurements in a diatom winter/spring bloom. Mar. Ecol. Prog. Ser. **54:** 109–119.

RUIZ, J. 1996. The role of turbulence in the sedimentation loss of pelagic aggregates from the mixed layer. J. Mar. Res. **54:** 385–406.

———, C. M. GARCIA, AND J. RODRIGUEZ. 1996. Sedimentation loss of phytoplankton cells from the mixed layer: Effects of turbulence levels. J. Plankton Res. **18:** 1727–1734.

SHERMAN, B. S., I. T. WEBSTER, G. J. JONES, AND R. L. OLIVER. 1998. Transitions between *Aulacoseira* and *Anabaena* dominance in a turbid river weir pool. Limnol. Oceanogr. **43:** 1902–1915.

SMAYDA, T. J. 1970. The suspension and sinking of phytoplankton in the sea. Oceanogr. Mar. Biol. Ann. Rev. **8:** 353–414.

SMETACEK, V., AND U. PASSOW. 1990. Spring bloom initiation and Sverdrup's critical-depth model. Limnol. Oceanogr. **35:** 228–234.

SMITH, I. R. 1982. A simple theory of algal deposition. Freshw. Biol. **12:** 445–449.

SPIGEL, R. H., AND J. IMBERGER. 1987. Mixing processes relevant to phytoplankton dynamics in lakes. N.Z. J. Mar. Freshw. Res. **21:** 361–377.

SVERDRUP, H. U. 1953. On conditions for the vernal blooming of phytoplankton. J. Cons. Int. Explor. Mer **18:** 287–295.

TENNEKES, H., AND J. L. LUMLEY. 1994. A first course in turbulence. 2nd ed. MIT Press.

THOMAS, G. B., AND R. L. FINNEY. 1988. Calculus and analytical geometry, 7th ed. Addison-Wesley.

VISSER, P. M., B. W. IBELINGS, B. VANDERVEER, J. KOEDOODS, AND L. J. MUR. 1996*a*. Artificial mixing prevents nuisance blooms of the cyanobacterium *Microcystis* in Lake Nieuwe Meer, The Netherlands. Freshw. Biol. **36:** 435–450.

———, L. MASSAUT, J. HUISMAN, AND L. R. MUR. 1996*b*. Sedimentaiton losses of *Scenedesmus* in relation to mixing depth. Arch. Hydrobiol. **136:** 289–308.

WAITE, A. M., AND S. D. NODDER. 2001. The effect of in situ iron addition on the sinking rates and export flux of Southern Ocean diatoms. Deep Sea Res. II **48:** 2635–2654.

———, P. K. BIENFANG, AND P. J. HARRISON. 1992. Spring bloom sedimentation in a subarctic ecosystem I. Nutrient sensitivity. Mar. Biol. **114:** 119–129.

WALLACE, B. B., D. P. HAMILTON, AND J. C. PATTERSON. 1996. Response of photosynthesis models to light limitation. Int. Rev. Ges. Hydrobiol. **81:** 315–324.

WALSBY, A. E. 1997. Numerical integration of phytoplankton photosynthesis through time and depth in a water column. New Phytol. **136:** 189–209.

WANG, L.-P., AND D. E. STOCK. 1993. Dispersion of heavy particles by turbulent motion. J. Atmos. Sci. **50:** 1897–1913.

WEBSTER, I. T., AND P. A. HUTCHINSON. 1994. Effect of wind on the distribution of phytoplankton cells in lakes revisited. Limnol. Oceanogr. **39:** 365–373.

———, G. J. JONES, R. L. OLIVER, M. BORMANS, AND B. S. SHERMAN. 1996. Control strategies for cyanobacterial blooms in weir pools. Murray-Darling Basin Commission technical report, NRMS project M3116 final report. CSIRO Land and Water Division, Canberra, Australia. T119.

YAMAZAKI, H., AND D. E. KAMYKOWSKI. 1991. The vertical trajectories of motile phytoplankton in a wind-mixed water column. Deep-Sea Res. **38:** 219–241.